ORIGINAL PAPER

Electrical resistivity imaging and engineering geological investigation of Gereb Segen dam, northern Ethiopia

Gebreslassie Mebrahtu[1] · Asmelash Abay[1] · Gebrerufael Hailu[2] · Miruts Hagos[1]

Abstract

The paper presents results of electrical resistivity imaging and engineering geological investigations conducted at the Gereb Segen dam site and reservoir to evaluate water tightness and stability. A programme of 2D resistivity imaging, discontinuity surveying, core drilling and Lugeon testing was conducted to assess the engineering geological performance of the dam and reservoir area. The geology of the dam site comprises alluvial deposits, dolerite, micritic limestone and marl-limestone-shale intercalation units. The investigations revealed dissolution cavities up to meters in size showing a preferred alignment along the valley; the separate lines of investigation correlated well to provide confidence in the findings. A karstified zone was identified at the base of the marly limestone unit at the dam site. A layer of gypsum found at shallow depth (9.5 m) along the dam axis may pose a dissolution hazard to water tightness and ground quality. Lugeon test results define very-low- to low-permeability units (shale with gypsum lenses and shale-mudstone) and high-permeability units (marly limestone and dolerite) and very-high-permeability zones associated with the karstic features. The presence of discontinuities and/or weak zones at the abutments and cavities at the dam foundation will affect the stability of the dam and facilitate leakage. Multiple line grout curtains for the karst zones and grouting for the jointed limestone at the dam axis and both abutments are recommended to reduce the possible leakage that will occur at the dam.

Keywords Engineering geology · Electrical resistivity imaging · Lugeon test · Leakage · Gereb Segen dam · Northern Ethiopia

Background

Gereb Segen dam is located 17 km southwest of Mekelle, capital city of Tigray regional state, northern Ethiopia and bounded by geographic coordinates 540,000 m to 545,000 m E and 1,479,700 m to 1,483,900 m N (UTM Zone: 37, Datum: Adindan) (Fig. 1). The embankment dam is 51 m high with a crest length of 850 m and reservoir capacity of 31 million m^3 and is designed to provide water supply to Mekelle city.

✉ Gebreslassie Mebrahtu
  gebreslassie.mebrahtu@mu.edu.et

1 School of Earth Sciences, Mekelle University, P.O. Box 231, Mekelle, Ethiopia

2 Institute of Geo-information and Earth Observation Sciences, Mekelle University, 231 Mekelle, Ethiopia

During the initial phase of construction, critical geological problems in relation to water tightness were identified. This research is aimed at addressing the geological challenges (water tightness and stability) of the dam site using geophysical and engineering geological investigations. The reservoir capacity of Gereb Segen dam is large compared to other micro-dams around the study area.

The variability in rainfall together with the extended duration of drought is threatening food and water security in Sub-Saharan Africa in general and East Africa in particular (De Hamer et al. 2008). Construction of dams in arid and semi-arid areas such as northern Ethiopia, where the main socioeconomic activity is rain-fed agriculture, is important and is directly linked to the erratic and variable rainfall (Yazew 2005; Walraevens et al. 2009). Northern Ethiopia, particularly the Tigray region, is often affected by drought largely as a result of uneven distribution of rainfall over many decades (Nedaw and Walraevens 2009; Berhane et al. 2013). One possible strategy for alleviating such a problem is through the use of various means of harvesting water for irrigation and drinking purposes. To this end, many water storage schemes have been
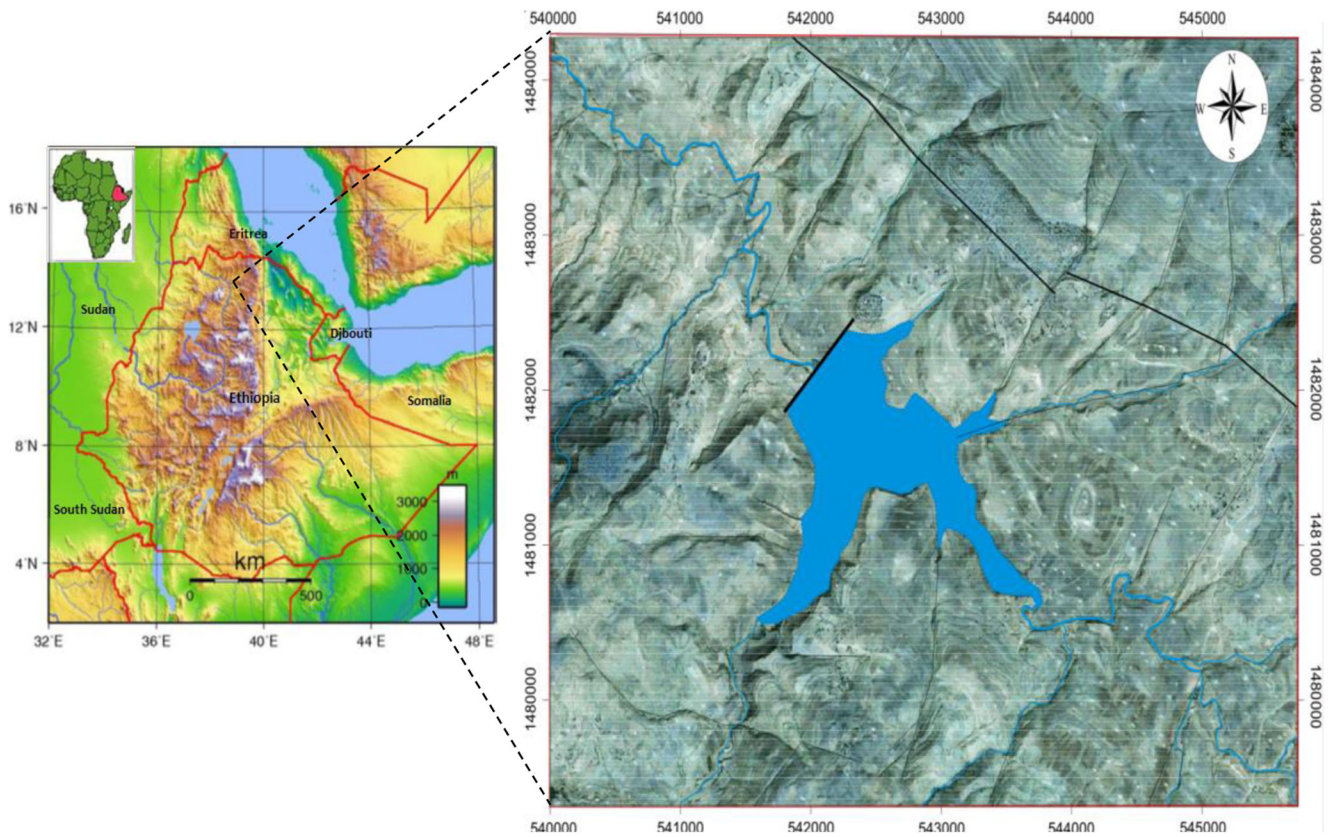
Fig. 1 Location map of Gereb Segen dam site with reference to Ethiopia and Africa. The location map is extracted from SPOT imagery

undertaken by the Regional Water Bureau and Federal Ministry of Water Resources over the past 15 to 20 years through the construction of micro-dam reservoirs. However, many of the micro-dams have failed to store the expected amount of water. This is mainly due to lack of engineering geological, geophysical and geotechnical investigations prior to dam construction (Haregeweyn et al. 2005; Abdulkadir 2009; Berhane 2010a, b).

One of the challenges faced by designers and development planners is the absence of basic and systematic data related to ground conditions for structures such as dams. Engineering geological investigation plays a significant role in the design and execution of such civil engineering projects (Panda et al. 2014; Rahimi et al. 2014), as it aims to gain an understanding of the interrelationships between the geological environment and the engineering situation, the nature and relationships of the individual geological components, the active geodynamic processes, and the likely results of the changes being made (UNESCO 1976).

In the past two decades, more than 70 earthfill dams have been constructed in the Tigray regional state, mainly for irrigation purposes (Abay and Meisina 2015). Of these, nearly 60% of the dams located in the Mekelle Outlier are subject to serious leakage through the reservoir and dam foundation (Haregeweyn et al. 2006; Berhane et al. 2013). Half of the leaking dams rest on systematically jointed carbonate rocks

(limestone and marl). According to Berhane et al. (2013), the limestone-marl intercalation unit with hydraulic conductivity of 10^{-6} to 1 m/s was found to be responsible for the excessive leakage of Hashenge and Arato micro-dams. According to Haregeweyn et al. (2006), ten micro-dams constructed on the shale-marl-limestone intercalation around Gereb Segen dam are characterized by very high leakage and become empty shortly after rainfall, as indicated in Table 1.

However, many dams have been built in carbonate foundations. Due to unknown karstic heterogeneity, many operating dams have leakage problems, e.g. Hales Bar Dam, USA (Lienhart 2013), Anchor Dam, USA (Jarvis 2003), Kalecik Dam, Turkey (Turkmen 2003), Mosul Dam, Iraq (Al-Saigh et al. 1994), Tangab Dam, Iran (Karimi et al. 2005; Mohammadi and Raeisi 2007) and Lar Dam (Uromeihy 2000). In carbonate terrane, karstification readily exploits the fractures and open structures developed as a result of valley stress relief and results in leakage of water from impoundment structures. Karst heterogeneity can be found on the surface (sinkholes) and in the subsurface (caves). The water leakage at Lar Dam is mostly due to the abundance of caves and conduits in the underlying limestone beds. Although many efforts have been made to prevent the leakage (mainly by grouting), none of these efforts have been successful (Uromeihy 2000). To investigate leakage problems, geotechnical (Bedmar and Araguas 2002; Milanovic

Table 1 Reservoir leakages in sedimentary basin of Mekelle Outlier (Haregeweyn et al. 2006)

Micro-dam	UTM location (Zone 37)		Reservoir capacity (m³)	Potential evaporation (m³)	Seepage loss (m³)	Seepage loss (%)
	Easting (m)	Northing (m)				
Adi-Akhor	565,580	1,484,813	291,138.9	25,095.75	265,683.2	91
Adi-Hilo	561,291	1,486,131	59,552.46	5143.85	53,958.6	91
Maytuwaru	563,738	1,487,881	84,898.65	5555.74	78,802.9	93
Era Quihila	564,688	1,486,570	675,450	81,185.2	144,517.2	21
Gereb-Beati	551,339	1,486,555	855,000	101,591.6	90,000	11
Gereb-Awso	560,089	1,485,026	614,004	8343.4	92,770	15
Adi-Eray	564,353	1,487,125	40,950	4656.8	35,348.23	86
Adi-Seleste	555,877	1,486,255	50,399.97	6566.07	42,933.9	85
Godew	559,271	1,486,227	91,000	10,420.5	79,769.5	88
Mokoro	562,560	1,488,291	31,920	4044.9	26,795.13	84

2004) and geophysical methods (Al-Fares 2011; Al-Saigh et al. 1994) must be applied.

Geological setting

Regional geology

The regional geology of northern Ethiopia has been studied at regional scale (e.g. Levitte 1970; Beyth 1971, 1972; Kazmin 1972; Garland 1980; Bosellini et al. 1997) and can be broadly divided into three major groups: the Neoproterozoic basement complex, Paleozoic-Mesozoic sedimentary sequences and Cenozoic trap volcanics (Levitte 1970). The Neoproterozoic basement complex of Mekelle area is the southern extension of the Arabian-Nubian Shield (ANS). It is composed of two major sequences (Beyth 1971): the Tsaliet Group, an older, mainly metavolcanic/volcaniclastic sequence; and the Tambien Group (Alene et al. 2006), a younger sediment-origin, low-grade metamorphic rock. Both groups are later intruded by syn- to post-tectonic intrusions, mainly granitic to granodioritic positions. The supracrustal metavolcanics/volcaniclastics contain intra-layer immature sediments mostly metamorphosed in the greenschist facies (Avigad et al. 2007). The magmatic-origin Tsaliet Group is composed mainly of intermediate to felsic and pyroclastics (welded tuffs, well-bedded lapilli tuffs and agglomerates; Beyth et al. 2003). The Tambien Group is exposed in many localities of the region. It is composed of mainly metasediments including slates, phyllites, graywackes, limestone/dolostone and diamectites/pebbly slates. Typical sections are defined in the Mai Kenetal and Negash synclinoria (Beyth et al. 2003). Late to post-tectonic granitoids, which are less deformed, frequently

intrude the metasediments (i.e., May Kinetal and Yechilla intrusions) with the exception of the Negash granitoid mainly intruding the metavolcanics/volcaniclastics. At few locations, small stocks of porphyritic diorite intrude the upper parts of the sequence (Beyth et al. 2003 and references therein).

The sediments in the Mekelle Outlier began to be deposited around the Ordovician or Carboniferous and probably ended in the Lower Cretaceous before the eruption of the Trap volcanics (Beyth 1971). The sedimentary rocks unconformably overlie the Neoproterozoic basement complex and form a nearly circular outlier 8000 km² in area around Mekelle. The Paleozoic sediments are the characteristic formation of northern Ethiopia, and can be subdivided in two unconformably bounded units, the Enticho sandstone and the Edaga Arbi glacials (Alemu et al. 2018). The Enticho sandstone comprises a cross-stratified quartz sandstone (quartz arenite; Avigad et al. 2007 and references therein) that locally contains varying size and composition conglomerate layers, and may be partially glacial in its upper part. Spatially, the rocks show wide thickness variation: from ~220 m to few meters. Unconformably overlying the Enticho sandstone and in some places the basement rocks, there are glaciogenic sediments (Edaga Arbi glacials) of predominantly dark-brown to light-red laminated/friable shale and siltstone which often contain dispersed pebbles or boulders, and minor diamictites (Bussert 2010).

The Mesozoic sedimentary rocks of the Mekelle basin form one of the best exposed basins in Ethiopia, constituting a nearly complete stratigraphic succession: from the lower Adigrat sandstone, through Antalo limestone to the Agula shale and Ambaradam sandstone. The Adigrat sandstone, lying unconformably on the Edaga Arbi glacial deposit, consists of up to 630 m of continental to shallow-marine siliciclastic sediment (Blanford 1869). It is fine–medium-grained, well-sorted and

mature sandstone capped at each major deposition by highly lateritized clastic layers. Interpretation of a depositional environment for this unit is controversial as most previous studies (e.g., Assefa 1991; Bosellini et al. 1997) consider the Adigrat sandstone as fluviatile. However, Dawit (2010) reported that the depositional environment is characteristic of tide-dominated estuarine conditions. The Antalo Formation, a major stratigraphic unit of the Mekelle Outlier, is characterized by the intercalation of limestone, marl and shale units. Based on the field observations and dominancy of the layers, the Antalo Formation is grouped into three categories, namely as marl-limestone-shale, limestone-marl and shale-marl-limestone units. Some limestone layers have shown signatures of small-scale karstification. The Antalo Formation (limestone) is conformably overlain by the Agula Shale Formation (Bosellini et al. 1997) which is composed of shale

with minor intercalations of marly limestone, mudstone and gypsum layers. At the central part of the outlier, the shale is intensively injected by sills and dikes (Fig. 2). The dikes and sills known as Mekelle dolerites are the youngest intrusive rocks. About 75% of the Mekelle Outlier is covered by the Antalo Formation and Agula shale with gypsum intercalations. The remaining part is covered by sandstones units (Adigrat and Ambaradam units).

At the top of the Mesozoic succession, there is a detrital and mottled sandstone called Ambaradam sandstone (Estifanos et al. 2018) which consists of mudstone, siltstone and pebbly sandstone. After a major unconformity, the Mesozoic succession of northern Ethiopia is covered by a 2-km-thick pile of flood basalt (Hagos et al. 2010; Ukstins et al. 2002). Lavas of this province erupted ~30 Ma ago, during a short period of 1–2 Ma, to form a huge volcanic plateau (Hofmann et al. 1997;
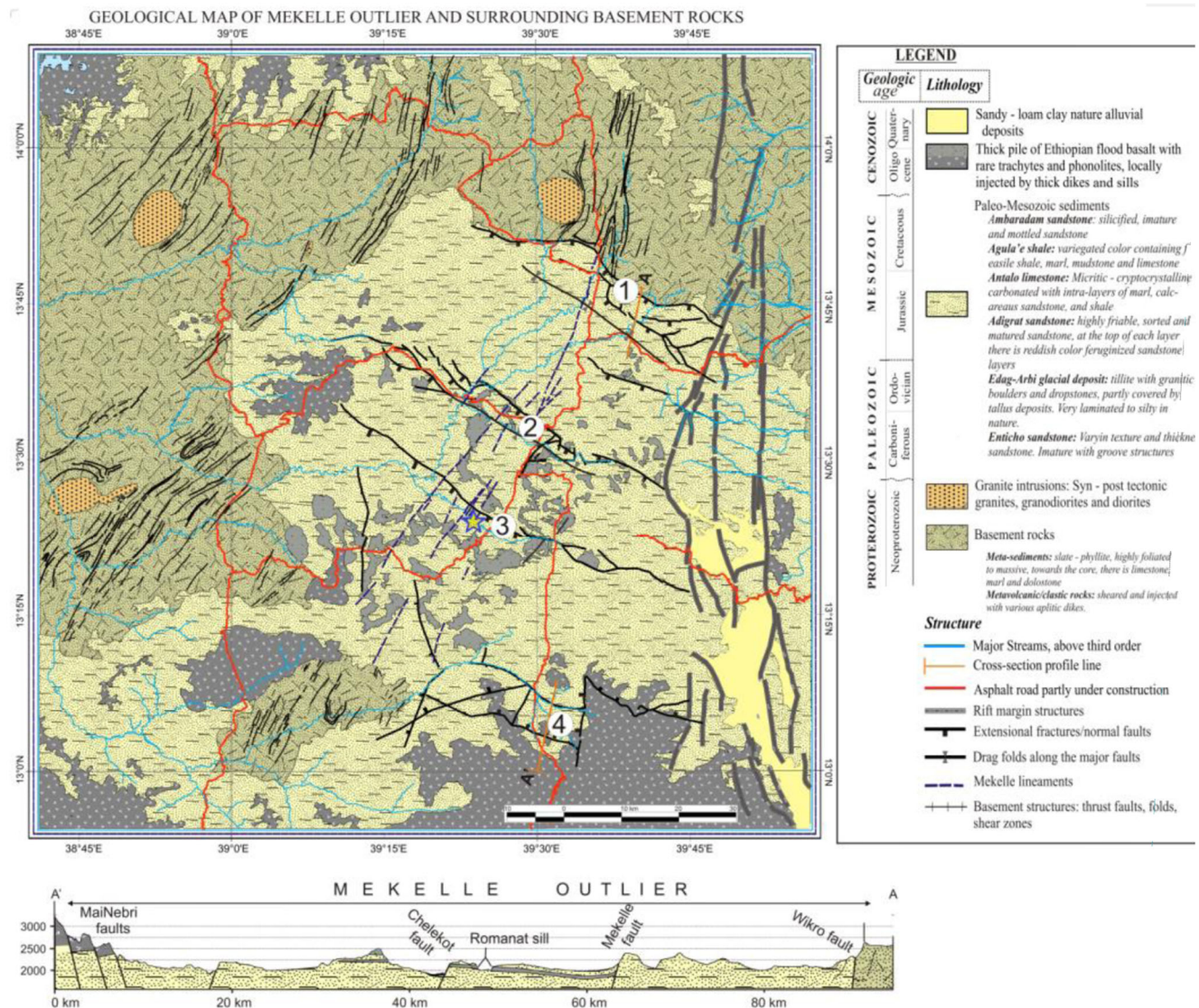

Fig. 2 Simplified geological map of central and eastern Tigray, northern Ethiopia. Circled numbers denote major WNW–ESE-trending fault zones: 1 = Wikro fault zone; 2 = Mekelle fault zone; 3 = Chelekot fault zone and 4 = Fursa Mariam fault zone. The yellow star indicates the site of the dam

Kieffer et al. 2004). The Mekelle Outlier is bounded to the north and south by Wikro and Fursa Mariam extension faults, respectively. At its center, the Mekelle and Chelekot faults cut the outlier into three blocks (Fig. 2).

Geology of the dam site

The dam site is covered by four geological units, namely alluvial deposits, dolerite, micritic limestone and marl-limestone-shale intercalation units (Fig. 3) as outlined below. The local geological units are correlated with the regional geology of northern Ethiopia. The alluvial deposit is correlated with Quaternary deposit, dolerite with Mekelle dolerite, micritic limestone and marl-limestone-shale intercalation with the Antalo limestone formation regionally.

Alluvial deposits cover the central part of the dam site in the valley floors along the main river and its tributaries (Fig. 3). This unit is composed of clay soil with units of gravel, with boulder-sized dolerite and limestone clasts. It has 10 m thickness at the center of the reservoir, but decreases towards the abutments. Dolerite is exposed as a sill in the right and left abutments, upstream and reservoir rim of the dam site. It is overlain by relatively jointed micritic limestone (Fig. 3). The thickness of the sill varies from 40 m to 50 m in the study
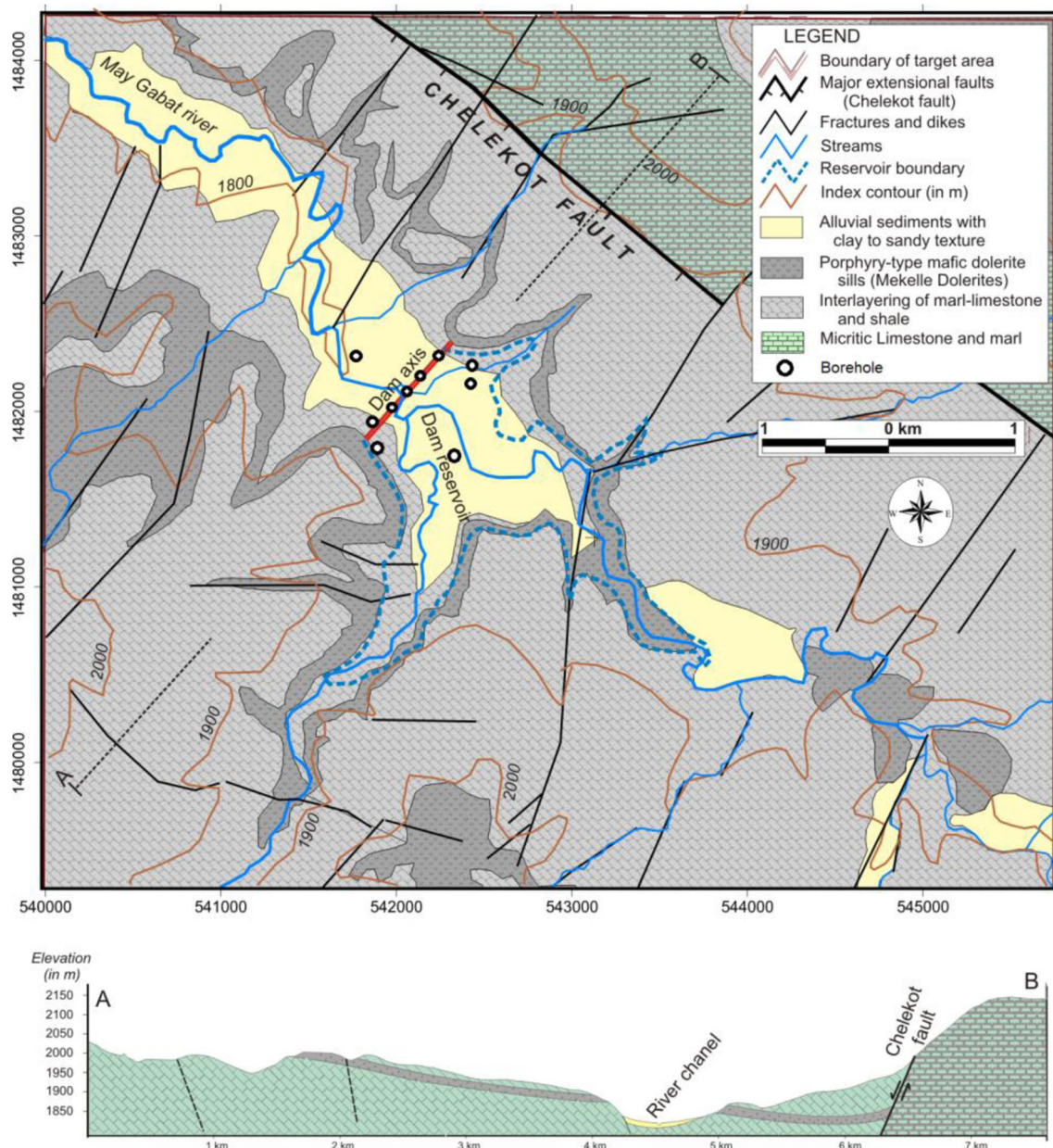

Fig. 3 Geological map of Gereb Segen dam site and its surrounding area. Lithologic contacts were extracted from SPOT imagery

area. The dolerite is highly weathered and shows exfoliation and spheroidal weathering (Fig. 4a). It shows dark-gray to black color and consists of medium- to fine-sized minerals.

A micritic limestone unit is found at the upper part of the left and right abutments and along the upper face of the reservoir rim. The field investigation showed that it is moderately to highly jointed (Fig. 4b). The aperture of the joints varies from 2 to 15 cm with an average joint spacing ranging from 50 to 125 cm without filling materials. Karstification in limestone is common in the downstream of the proposed dam site. A highly weathered marl-limestone-shale intercalation unit is also observed in both right and left abutments and downstream of the dam.

Materials and methods

Electrical resistivity imaging

Electrical resistivity method has advanced from conventional vertical sounding to 2D and 3D resistivity imaging, which can provide high-resolution electrical images (Colella et al. 2004). 2D electrical resistivity imaging was executed with the objective of determining the nature and thickness of the subsurface units and to detect geological weak zones like dykes, faults, cavities and fissures at the dam site. In the present study, 2D resistivity imaging was carried out using a Wenner array and ABEM Terrameter SAS 4000 (ABEM 1999, 2012). The data was processed using the RES2DINV package (GeoTomo Software, Loke 2001) to create a 2D resistivity model using the inverted apparent resistivity values (Griffiths and Barker 1993). The program makes use of the least-squares method based on a quasi-Newton optimization technique (Loke and Barker 1996; Dahlin 1996).

Four profiles (Fig. 5) of electrical resistivity imaging were selected at the dam site. Profile 1 (SW-NE) was conducted along the dam axis with 20 m electrode spacing covering a total length of 780 m (Fig. 4a). The maximum depth of investigation in this, and all other profiles, reached 25.5 m. Profile 2 (SE-NW) was oriented perpendicular to the dam axis covering a total length of 640 m with 20 m spacing between the electrodes (Fig. 5b). Profile 3 (NW-SE) was taken at the left reservoir rim of the rim site where lineaments were detected from satellite imagery. The electrode spacing was the same as that of profiles 1 and 2 with a total length of 680 m (Fig. 5c). Profile 4 (NW-SE) was taken at the right reservoir rim of the dam with 20 m spacing and a total length of 380 m (Fig. 5d).
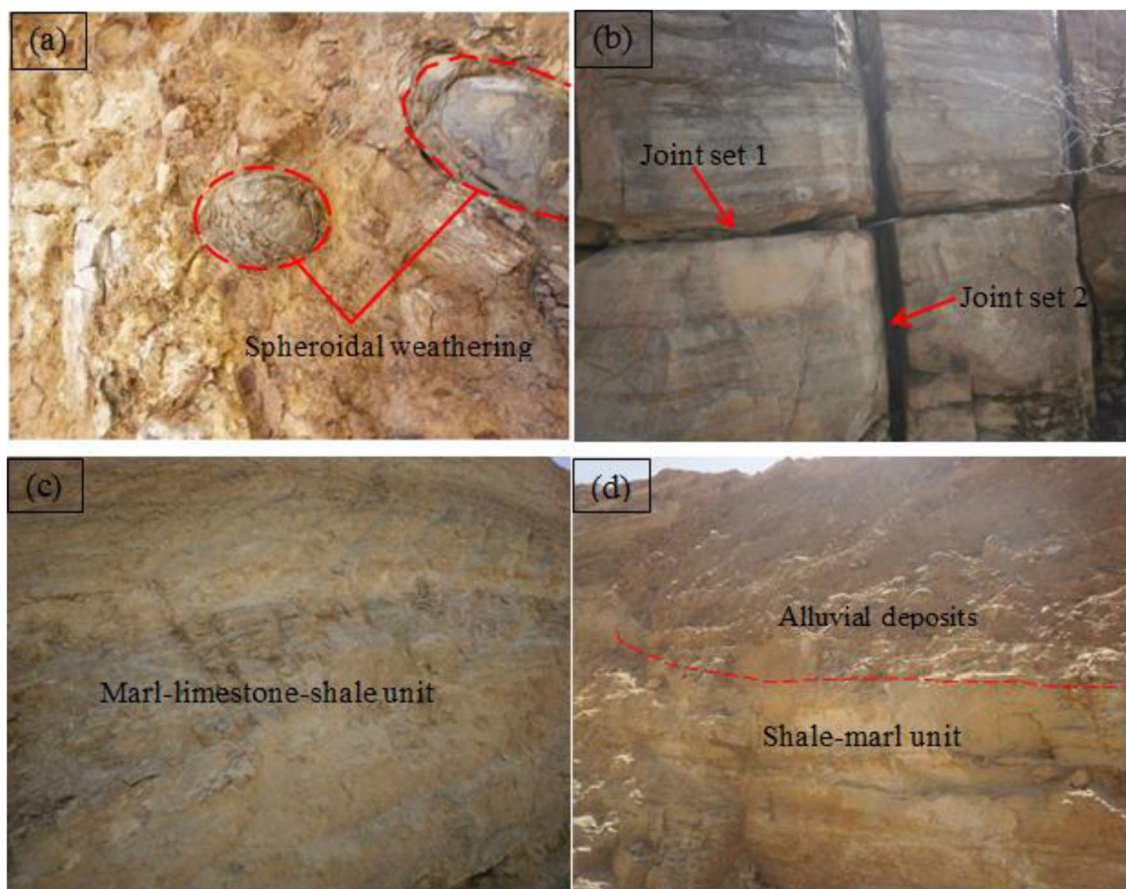

Fig. 4 **a** Spheroidal weathering of dolerite at the right abutment, **b** limestone outcrops, jointed in two sets at the right abutment of the dam, **c** marl-limestone-shale intercalation unit at the trench excavation of right abutment and **d** alluvial deposits overlying shale-marl unit
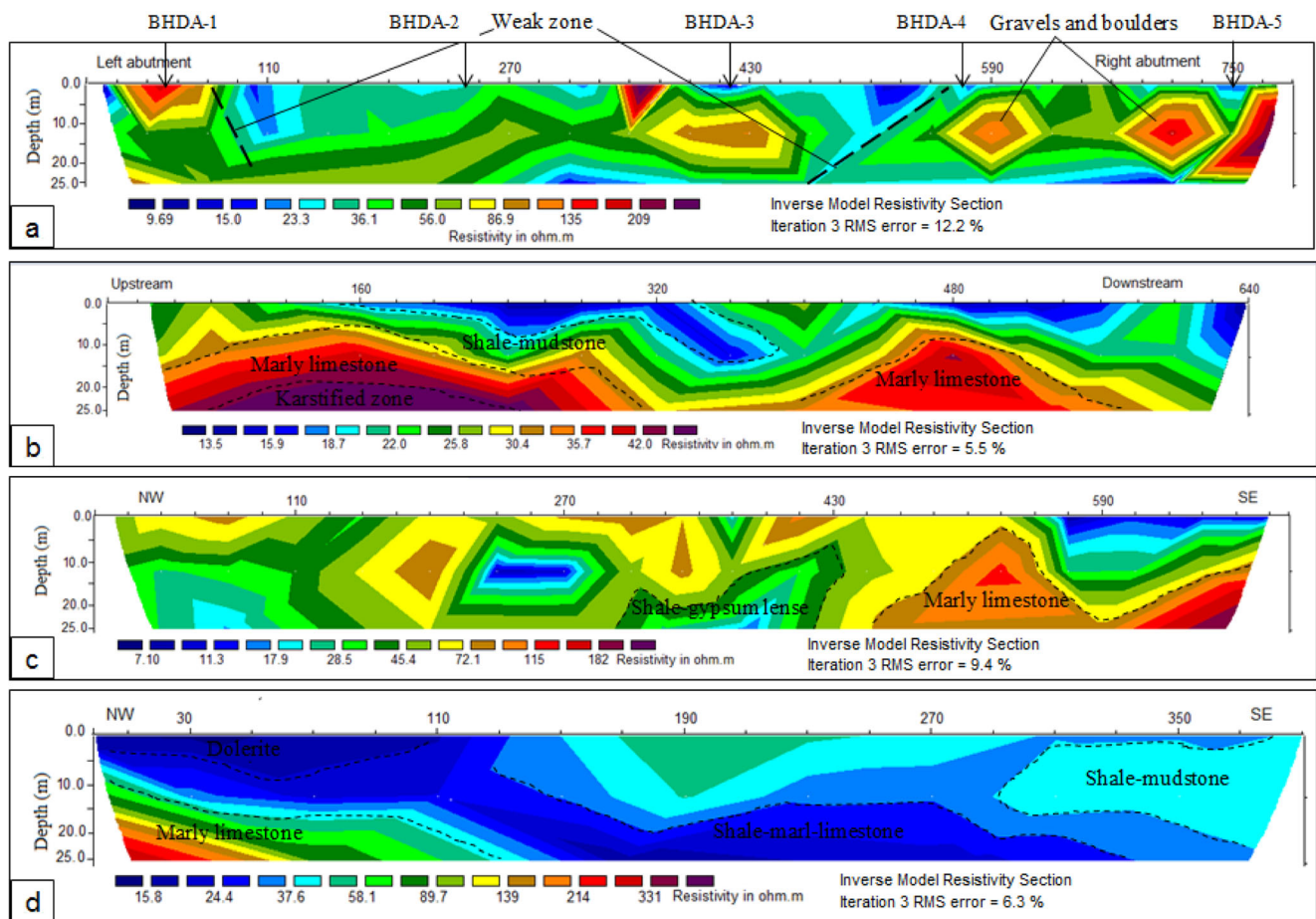
Fig. 5 Inverse model resistivity imaging sections of four profiles: **a** profile 1, **b** profile 2, **c** profile 3, and **d** profile 4

Engineering geological investigation methods

The engineering geological investigations of the dam site include discontinuity surveying, core drilling and Lugeon testing. A number of field observations and discontinuity measurements were recorded at the dam site in accordance with the suggested method of the International Society of Rock Mechanics (ISRM 1981). The condition of major joint sets (orientation, spacing, persistence, roughness, aperture and filling) relative to an engineering structure largely controls the possibility of unstable conditions, excessive leakage and deformations (Maerz and Zhou 1999). A total of 117 discontinuities were recorded using a Brunton compass on the left and right banks. Discontinuity orientations were processed using a RockWorks15 linear rose diagram (RockWare Inc. 2009) (Fig. 6).

Ten borehole locations were selected based on the geological conditions, topography and geophysical survey of the dam site and drilled to a depth of 38–51 m, with a total core length of 451 m using NX wire line equipment (54.7 mm core diameter). The distribution of boreholes was: five at the dam axis, three at the reservoir, one at the spillway route and one at

downstream part of the dam (Fig. 3). Rock quality designation (RQD, Deere 1968) and rock mass rating (RMR, Bieniawski 1989) were calculated from the drill cores to characterize rock mass quality at the dam site.

A total of 33 Lugeon tests were conducted in ten boreholes to assess the permeability of the rocks. The testing was carried out at intervals along the boreholes with the testing section sealed off by inflatable packers. The maximum test pressure was defined before commencing the test, and pressure stages were lowered after using maximum pressure (Quiñones-Rozo 2010; Öge 2017). The data obtained from boreholes were used directly to assess leakage risks, and compared indirectly with the data from the resistivity imaging profiles.

Results and discussion

2D electrical resistivity imaging

The inverse model resistivity profiles show variable resistivity values both laterally and vertically (Fig. 5). The obtained root

Fig. 6 Rose diagram of dominant joints at the **a** right abutment and **b** left abutment of the dam site
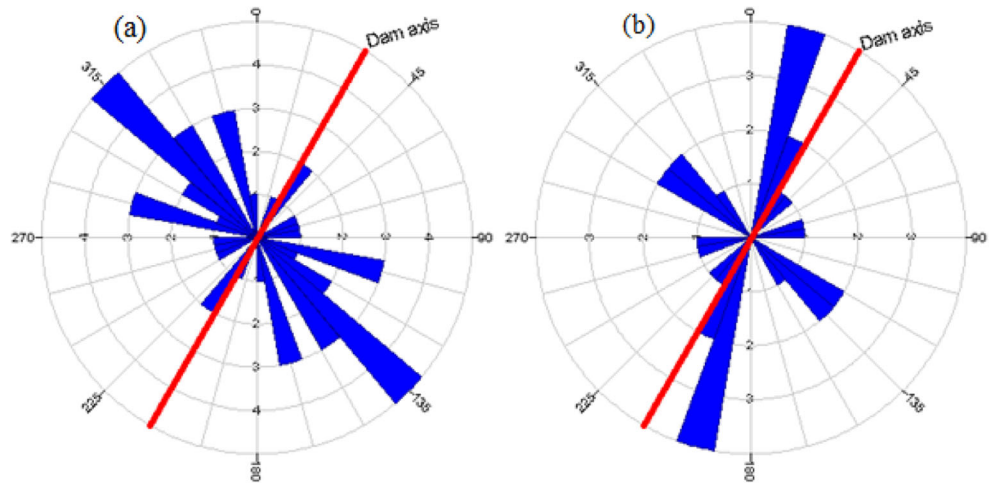
mean square errors of the four profiles (1, 2, 3 and 4) are 12.2%, 5.5%, 9.4% and 6.3%, respectively. The 2D imaging section in Fig. 5a clearly depicts the lateral variations underlying the dam axis. The two abutments are characterized by resistivity values of 80 to 200 Ω.m, attributed to weathered dolerite and jointed black limestone. Near the central part of the dam axis (at around 430 m chainage) there are medium-resistivity (90 Ω.m) pockets at shallower depth, mainly attributed to alluvial boulders of the remnant buried channel. In the central part of the dam axis, the resistivity values of 36 Ω.m to 60 Ω.m are taken to represent interlayers of various resistivity values reflecting marl-limestone-shale intercalations. Figure 5a shows possible weak zones at chainages of 80 m and 560 m. Low resistivity values (15–23 Ω.m) at the bottom of the right abutment are identified as a shale-gypsum unit).

Profile 2 taken upstream-downstream (Fig. 5b) shows three major geological layers which correlate with the geological cross section (Fig. 7b) produced from the drilling tests. The top layer with low resistivity (13.5–20 Ω.m) is fine to coarse alluvial deposits underlain by a more resistive (22–30.4 Ω.m) layer of marl-limestone-shale. The third layer is more resistive with resistivity values ranging from 32 Ω.m to >42 Ω.m, representing a marly limestone unit. Towards the downstream, the resistivity values become high, while in the central part they are low, related to fine alluvial deposits to a depth of 10 m. The bottom part in the upstream of the dam recorded high resistivity (>45 Ω.m) which is interpreted as an air-filled karstified zone (Fig. 5b), as later confirmed by borehole drilling (Fig. 7c). It is common that cavities present at shallow depths above the water table in semi-arid areas that are filled
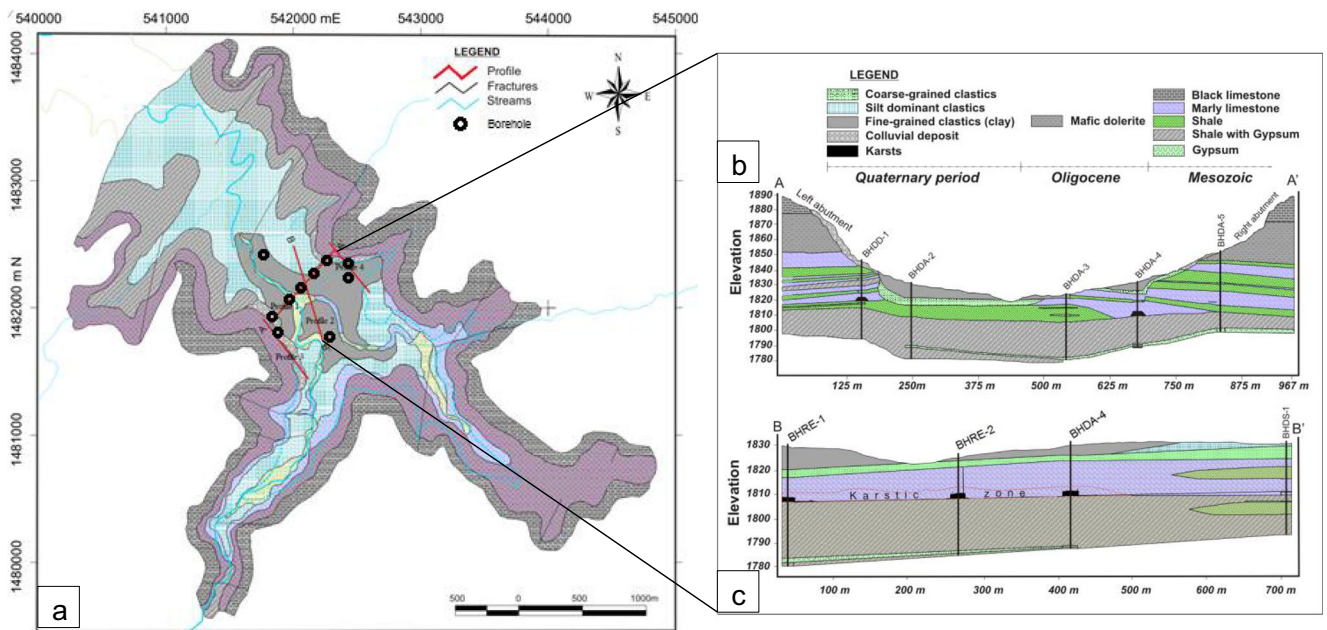

Fig. 7 **a** Engineering geological map of the dam site, **b** geological cross sections along the dam axis (A-A' section) and **c** upstream-downstream (perpendicular to dam axis) (B-B' section). Electrical profiles (profiles 1, 2, 3 & 4) are indicated in red line

by air (not by groundwater) produce high electrical resistivity values (Martínez-Pagán et al. 2013).

The 2D resistivity imaging along the left reservoir periphery (Fig. 5c) near the spillway is characterized by variable resistivity values due to the presence of heterogeneous units such as weathered dolerite, fractured limestone and disturbed shale-marl-limestone intercalations. The thickness of the top layer shows medium resistivity (60–90 Ω.m) which increases from the northwest to southeast part of the left reservoir. But, its resistivity drops at chainage distance of 570 m onward towards the southeast corner. Figure 5d shows two layers along the right reservoir rim. The top thin layer is dominated by shale-mudstone towards the southeastern part and highly weathered dolerite in the northwestern part which exhibits low resistivity. The bottommost part of the NW direction is characterized by moderate to hard marly limestone.

Engineering geological investigations

Discontinuity surveys

Detailed discontinuity surveys were executed for the rocks outcropping in the dam site to examine the rock mass quality and their influence on the water tightness. Of the 117 discontinuity measurements recorded in the dam area, 28 were from the left abutment and 89 from the right abutment. Two sets of joints orienting NW-SE and NE-SW dominate on both the left and right abutments (Fig. 6). The NW-SE-trending joints are a potential route for reservoir water leakage as they are subparallel to the likely flow direction. The joints are mostly smooth, narrow apertures (2–15 cm), and joint spacing ranges from 50 cm to 125 cm. Moreover, some wedge failures were observed in both abutments and reservoir rim following the intersection of these joints.

Core drilling

Borehole sites were selected following the electrical resistivity imaging survey and surface geological mapping. From the borehole drilling, lithological cross sections (Fig. 7b) were prepared to understand the vertical and lateral variation of strata. Rock quality designation (RQD) (Deere 1968) is calculated for the rock units present in the dam site (Table 4). The RQD value for black limestone exposed at the rim of the reservoir is estimated from the surface measurements using a volumetric joint count (Palmstrom 1974), while the RQD of other rocks is estimated for the borehole core samples as shown in Table 2. Accordingly, the RQD values for the rock masses at both abutments are lower than at the central foundation. Thus, rocks at the two abutments are liable to exhibit excessive leakage and stability problems.

As shown in Fig. 7b, the top layer of the central foundation of the dam is covered by alluvial soils (clay, sand and gravel) and underlain by shale and marly limestone units. The weathered dolerite about 25–30 m thick, observed in both left and right abutments, is overlain by massive black limestone. A shale-gypsum unit is the bottommost unit ranging in thickness from 11 m in borehole BHDA-5 to 29 m in BHDA-2. A pure gypsum layer (0.5–1.5 m thick) is also detected in four boreholes (BHDA-2, BHDA-3, BHDA-4 and BHDA-5) (Fig. 7b). Occurrence of gypsum at shallow depth (9.5 m) along the central foundation in borehole BHDA-3 may interact with percolating water through joints and dissolve easily to form small caves and sinkholes. This can allow excessive leakage and cause differential settlement of the dam.

The drilling results show that cavities having sizes of 2.5 m (21.7–24.2 m depth) and 3 m (17.25–20.25 m depth) are present along the dam axis as shown in BHDA-1 and BHDA-4 (Fig. 7b). Similarly, 0.8 m and 2.7 m cavities were observed in boreholes BHRE-1 and BHRE-2, respectively, along the reservoir perpendicular to the dam axis (Fig. 7c). Cavities were well developed in marly limestone because it is susceptible to dissolution when it is in contact with water. This implies that the marly limestone rock in the dam site and reservoir area is potentially affected by cavity formation, which in turn could give rise to excessive leakage and dam instability.

Permeability testing

A total of 33 Lugeon tests were carried out, and Lugeon values for different rock units are presented in Table 3. Results

Table 2 Average RQD values obtained for core samples from the left abutment (LF), right abutment (RA) and central foundation (CF) of Gereb Segen dam site

Rock type	BHDA-5 (RA)	BHDA−2,3,4 (CF)	BHDA-1 (LA)	Overall average RQD	RQD class (Deere 1968)
Black limestone	78	–	78	78	Good
Dolerite	15	–	–	15	Very poor
Shale-mudstone	24	56	10	38	Very poor
Marly limestone	27	48	18	43	Poor
Shale gypsum lens	65	74	50	67	Fair
Gypsum	85	92	–	88	Good

Table 3 Average Lugeon values for different rock masses at Gereb Segen dam site

Rock type	Lugeon value (uL)			Hydraulic conductivity classification (Quiñones-Rozo 2010)	Rock mass discontinuity condition
	Minimum	Maximum	Average		
Black limestone	14	36	28	Medium	Some open
Marly limestone	18	131	56	High	Many open
Dolerite	30	96	65	High	Many open
Shale-mudstone	0.1	20	2.9	Low	Tight
Shale-gypsum lens	0.1	1	0.6	Very low	Very tight

revealed that permeability is high in marly limestone and dolerite units due to the presence of open fractures and a moderate degree of weathering. This may allow seepage through the abutments and central foundation of the dam. Rock masses having Lugeon values above 3 indicate a need for grouting treatment (Houlsby 1990). During the Lugeon test at the cavity section (e.g. BHDA-4), there was no permeability record as the pressure could not be developed due to complete water loss.

Shale-gypsum lenses and shale units are classified into very-low- and low-permeability zones, respectively. Though the permeability of shale-gypsum is low, the presence of very thin layers (3–10 cm) of gypsum may cause stability problems due to dissolution. Permeability tests were also conducted on alluvial soils, dominated by clay and silt. Falling-head permeability tests performed on fine-grained soils from three boreholes from the central foundation indicate low hydraulic conductivity ($1.06 * 10^{-6}$ m/s). Hydraulic conductivity generally decreases with depth due to the effect of overburden (Lee and Farmer 1993; Nappi et al. 2005) as shown in Fig. 8a, although exceptions were noticed. In three boreholes (BHDA-1, BHDA-4 and BHDA-5), the hydraulic conductivity value

Fig. 8 **a** Lugeon value versus depth for five boreholes drilled along dam axis. **b** Lugeon value contour map along the dam foundation
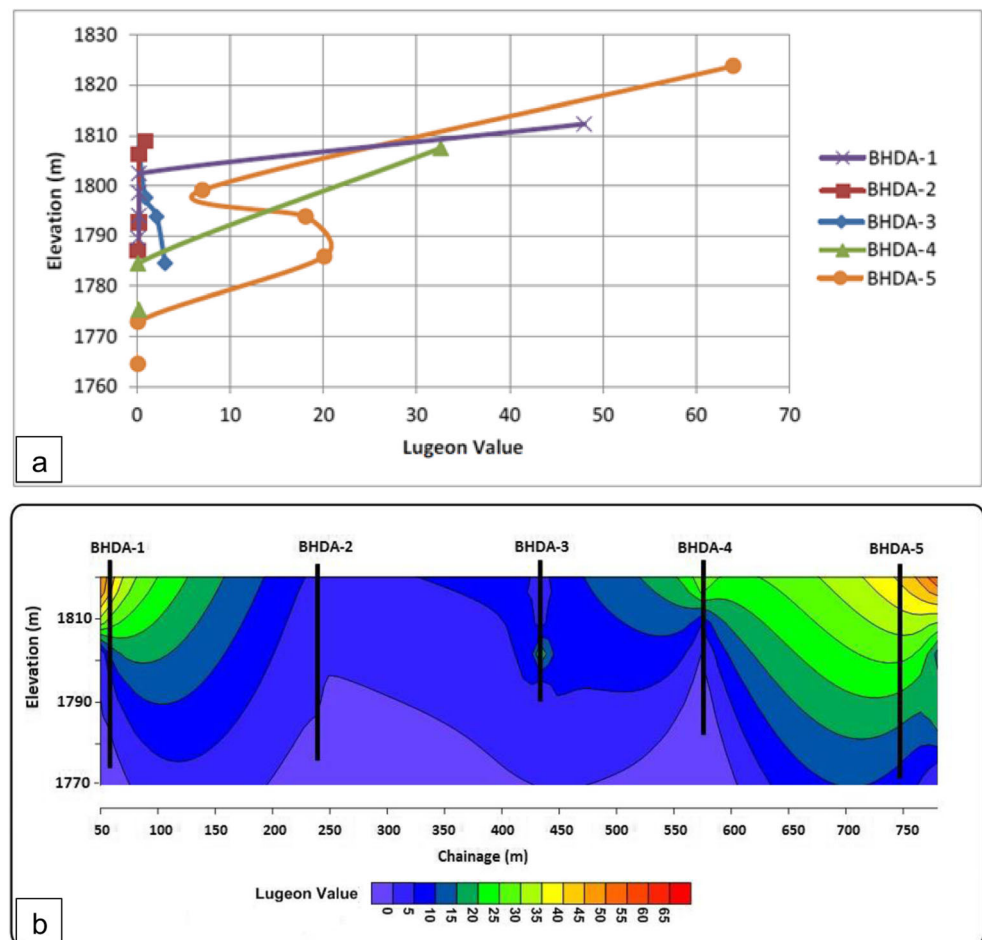
Table 4 RMR values of different rock masses at Gereb Segen dam site

Parameters	Black limestone		Marly limestone		Dolerite		Shale-mudstone		Gypsum	
	Value	Rating	Value	Rating	Value	Rating	Value	Rating	Value	Rating
Uniaxial compressive strength (MP)	55	7	51	7	35	4	12	2	28	4
RQD	78	17	43	8	15	3	38	8	88	17
Discontinuity spacing (mm)	635	15	450	10	210	10	165	8	320	10
Discontinuity condition	Rough, 3–10 m persistence, slightly weathered, >5 mm aperture with no infilling	18	Rough, 1–3 m persistence, slightly weathered, soft gouge >5 mm, 1–5 mm aperture	15	Very rough, <1 m persistence, highly weathered, 1–5 mm aperture with hard infilling >5 mm	16	Slightly rough, <1 m persistence moderately weathered, 1–5 mm aperture with soft infilling	15	Slightly rough, 1–3 m persistence, slightly weathered, >5 mm aperture, <5 mm soft infilling	14
Groundwater	Completely dry	15	Damp	10	Completely dry	15	Damp	10	Wet	7
Discontinuity orientation	Favorable	−2	Favorable	−2	Favorable	−2	Favorable	−2	Favorable	−2
RMR rating		70		48		46		41		50
RMR class		Good		Fair		Fair		Fair		Fair

decreases with increasing depth. But in two boreholes (BHDA-2 and BHDA-3), permeability is nearly constant with depth. From the Lugeon test results (Table 3), rocks near the central foundation, which is dominated by shale (2.9 uL) and shale-gypsum units (0.6 uL), show low and very low permeability, respectively. On the other hand, fractured marly limestone (56 uL) and weathered dolerite (65 uL) at the left and right abutments show high permeability (Fig. 8b), which could also be a possible source of leakage.

Rock mass classification

Rock mass classification is an important geological factor for the design and construction of a dam. It not only evaluates the properties of rock masses, but also helps in determining the range of utilizable rock masses around the dam and the reasonable excavation depth of the dam foundation (Lashkaripour and Ghafoori 2002). Rock mass classification is calculated according to rock mass rating (RMR, Bieniawski 1989). The rating of each RMR parameter is summed to obtain the total RMR value, as presented in Table 4. The rocks are thus classified in the range of good rock quality (class II) to fair rock quality (class III). Hence, the rock masses can serve as a foundation for the earth dam. However, treatment is needed to reduce the permeability of rock masses as the seepage is expected to be high which could create foundation stability problems.

Conclusions

In this study, 2D electrical resistivity imaging and engineering geological investigations were conducted to examine the subsurface geological formations at the dam site. The site is underlain by alluvial deposits, dolerite, micritic limestone and marl-limestone-shale intercalation units. Four cavities (two at the reservoir, one at the left abutment and one at the right central foundation) ranging in size from 0.8 m to 3 m were found at the dam site within the marly limestone layer, forming a karstified zone at the dam site. The presence of the karstified zone at the reservoir and dam foundation will likely lead to significant leakage for Gereb Segen dam. From this finding, it is possible to deduce that the marly limestone unit is expected to have similar cavities around the reservoir which could be the source of excessive water loss through the reservoir and foundation of the dam. Furthermore, the presence of soluble gypsum layers at a shallow depth (9.5 m) in the dam foundation could further threaten the stability of the structure of the dam in the long term due to its potential for dissolution. Lugeon test results indicate that the two abutments were characterized by high-permeability zones (56–65 uL) due to the fractured marly

limestone and weathered dolerite, while the central foundation is covered by low-permeability alluvial deposits underlain by an impervious shale unit. The results of the study show that the correlation between geophysical survey and subsurface investigation is satisfactory. For the karst zones at the foundation, a multiple-line grout curtain is recommended to reduce seepage losses, and grouting along the dam axis where jointed limestone is found. Additionally, blanketing of reservoir peripheries and the river bed is important.

References

Abay A, Meisina C (2015) Engineering-geological properties of carbonates and shale: their implications for dam construction in Mekelle, Northern Ethiopia. Momona Ethiop J Sci 7(1):64–84

Abdulkadir M (2009) Assessment of micro-dam irrigation projects and runoff predictions for ungauged catchments in northern Ethiopia (PhD Thesis), Muenster University, Germany

ABEM (1999) ABEM Terrameter SAS 4000/SAS 1000. Instruction manual. ABEM printed matter 93101. ABEM, Sweden

ABEM (2012) ABEM terrameter LS. Instruction manual. ABEM printed matter 20120109. ABEM, Sweden Based on release 1.10

Alemu T, Abdelsalam MG, Dawit EL, Atnafu B, Mickus KL (2018) The Paleozoic e Mesozoic Mekele Sedimentary Basin in Ethiopia: an example of an exhumed IntraCONtinental Sag (ICONS) basin. J Afr Earth Sci 143:40–58

Alene M, Jenkin GRT, Leng MJ, Darbyshire DPF (2006) The Tambien Group, Ethiopia: an early Cryogenian (ca. 800–735 Ma) neoproterozoic sequence in the Arabian–Nubian shield. Precambrian Res 149:79–89

Al-Fares W (2011) Contribution of the geophysical methods in characterizing the water leakage in Afamia B dam Syria. J Appl Geophys 75:464–471

Al-Saigh NH, Mohammed ZS, Dahham MS (1994) Detection of water leakage from dams by self-potential method. Eng Geol 37:115–121

Assefa G (1991) Lithostratigraphy and environment of deposition of the Late Jurassic-Early Cretaceous sequence of the central part of Northwestern Plateau, Ethiopia. Neues Jb Geol Paläontol Abh 182:255–284

Avigad D, Stern RJ, Beyth M, Miller N, McWilliams M (2007) Detrital zircon U–Pb geochronology of Cryogenian diamictites and lower Paleozoic sandstone in Ethiopia (Tigrai): age constraints on Neoproterozoic glaciation and crustal evolution of the southern Arabian–Nubian shield. Precambrian Res 154:88–106

Bedmar AP, Araguas L (2002) Detection and the prevention of leaks from dams. CRC Press, Boca Raton

Berhane G (2010a) Geological, geophysical and engineering geological investigation of a leaky micro-dam in the Northern Ethiopia. Agric Eng Int CIGR J 12(1):31–46

Berhane G (2010b) Engineering geological soil and rock characterization in the Mekelle Town, Northern Ethiopia: implications to engineering practice. Momona Ethiop J Sci 2(2):64–86

Berhane G, Martens K, Al Farrah N, Walraevens K (2013) Water leakage investigation of micro-dam reservoirs in Mesozoic sedimentary sequences in Northern Ethiopia. J Afr Earth Sci 79:98–110

Beyth M (1971) The geology of Central and Western Tigray. Unpub. Report. Ethiopian Institute of Geological Survey (EIGS), Addis Ababa

Beyth M (1972) Paleozoic sedimentary basin of Mekelle Outlier, Northern Ethiopia. Am Assoc Pet Geol Bull 56(12):2426–2439

Beyth M, Avigad D, Wetzel H-U, Matthews A, Berhe SM (2003) Crustal exhumation and indications for Snowball Earth in the East African Orogen: North Ethiopia and East Eritrea. Precambrian Res 123:187–201

Bieniawski ZT (1989) Engineering rock mass classifications. Wiley, New York, p 251

Blanford W (1869) On the geology of a portion of Abyssinia. Q J Geol Soc Lond 25:401–406

Bosellini A, Russo A, Fantozzi PL, Assefa G, Tadesse S (1997) The Mesozoic succession of the Mekele Outlier (Tigrai Province, Ethiopia). Memoir Sci Geol 49:95–116

Bussert R (2010) Exhumed erosional landforms of the Late Palaeozoic glaciation in northern Ethiopia: indicators of ice-flow direction, palaeolandscape and regional ice dynamics. Gondwana Res 18:356–369

Colella A, Lapenna V, Rizzo E (2004) High-resolution imaging of the High Agri Valley Basin (Southern Italy) with electrical resistivity tomography. Tectonophysics 386:29–40

Dahlin T (1996) 2D resistivity surveying for environmental and engineering applications. First Break 14(7):275–284

Dawit LE (2010) Adigrat Sandstone in Northern and Central Ethiopia: stratigraphy, facies, depositional environments and palynology. Ph.D. Thesis. Technische Universität, Berlin, 166p

De Hamer W, Love D, Owen R, Booij MJ, Hoekstra AY (2008) Potential water supply of a small reservoir and alluvial aquifer system in southern Zimbabwe. Phys Chem Earth 33:633–639

Deere DU (1968) Geological consideration. In: Stagg KG, Zienkiewicz OC (eds) Rock mechanics in engineering practice. Wiley, New York, pp 1–20

Estifanos S, Abay A, Hagos M, Mebrahtu G (2018) Assessing the aptitude of vesicular volcanic rock as pozzolanic sources for supplementary cementitious materials. Bull Eng Geol Environ 78(3):1607–1616

Garland CR (1980) Geology of the Adigrat Area. Geological Survey of Ethiopia Memoir 1, p. 51

Griffiths DH, Barker RD (1993) Two-dimensional resistivity imaging and modelling in areas of complex geology. J Appl Geophys 29:211–226

Hagos M, Koeberl C, Kabeto K, Koller F (2010) Geology, petrology and geochemistry of the basaltic rocks of the Axum area, Northern Ethiopia. In: Ray J, Sen G, Ghosh B (eds) Topics in igneous petrology. Springer, Netherlands, pp 69–93

Haregeweyn N, Poesen J, Nyssen J, Verstraeten G, de Vente J, Govers G, Deckers S, Moeyersons J (2005) Specific sediment yield in Tigray-Northern Ethiopia: assessment and semi-quantitative modelling. Geomorphology 69(1–4):315–331

Haregeweyn N, Poesen J, Nyssen J, De Wit J, Haile M, Govers G, Deckers S (2006) Reservoirs in Tigray (Northern Ethiopia): characteristics and sediment deposition problems. Land Degrad Dev 17(2):211–230

Hofmann C, Courtillot V, Feraud G, Rochette P, Yirgu G, Ketefo E, Pik R (1997) Timing of the Ethiopian flood basalt event and implications for plume birth and environmental change. Nature 389:838–841

Houlsby AC (1990) Construction and design of cement grouting: a guide to grouting in rock foundation. Wiley, New York

ISRM (1981) Suggested methods for the quantitative description of discontinuities in rock masses. Rock characterization, testing and monitoring. Pergamon, London 221 pp

Jarvis T (2003) The money pit: Karst failure of Anchor Dam, Wyoming. In: Evaporite Karst and engineering/environmental problems in the United States, 271–278. Oklahoma Geological Survey Circular 109

Karimi H, Raeisi E, Zare M (2005) Physicochemical time series of karst springs as a tool to differentiate the source of spring water. Carbonates Evaporites 20(2):138–147

Kazmin V (1972) Geological map of Ethiopia. EIGS, Addis Ababa

Kieffer B, Arndt N, Lapierre H, Bastien F, Bosch D, Pecher A, Yirgu G, Ayalew D, Weis D, Jerram AD, Keller F, Meugniot C (2004) Flood and shield basalts from Ethiopia: magmas from the African superswell. J Petrol 45:793–834

Lashkaripour GR, Ghafoori M (2002) The engineering geology of the Tabarak Abad Dam. Eng Geol 66:233–239

Lee CH, Farmer I (1993) Fluid flow in discontinuous rocks. Chapman & Hall, New York

Levitte D (1970) The geology of Mekele, report on the geology of the central part of sheet ND 37–11. Geological Survey of Ethiopia, Addis Ababa

Lienhart DA (2013) Long-term geological challenges of dam construction in a carbonate terrane. Environ Eng Geosci 19:1–25

Loke MH (2001) Tutorial: 2-D and 3-D electrical imaging surveys

Loke MH, Barker RD (1996) Rapid least-squares inversion of apparent resistivity pseudo sections using a quasi-Newton method. Geophys Prospect 44(1):131–152

Maerz NH, Zhou W (1999) Multivariate analysis of borehole discontinuity data. In: Rock mechanics for industry. Proceedings of the 37th US Rock Mechanics Symposium, Vail Colorado, vol. 1, pp 431–438

Martínez-Pagán P, Gómez-Ortiz D, Martín-Crespo T, Manteca JI, Rosique M (2013) The electrical resistivity tomography method in the detection of shallow mining cavities. A case study on the Victoria Cave, Cartagena (SE Spain). Eng Geol 156:1–10

Milanovic PT (2004) Water resources engineering in Karst. CRC Press LLC, Boca Raton

Mohammadi Z, Raeisi E (2007) Method of leakage study at karst dam sites: a case study: Khersan 3 Dam site, Iran. Environ Geol 52(6):1053–1065

Nappi M, Esposito L, Piscopo V, Rega G (2005) Hydraulic characterization of some arenaceous rocks of Molise (Southern Italy) through outcropping measurements and Lugeon tests. Eng Geol 81(1):54–64

Nedaw D, Walraevens K (2009) The positive effect of micro-dams for groundwater enhancement: a case study around Tsinkanet and Rubafeleg area, Tigray, northern Ethiopia. Momona Ethiop J Sci 1(1):59–73

Öge IF (2017) Assessing rock mass permeability using discontinuity properties. Procedia Engineering, Symposium of the International Society for Rock Mechanics. 191:638–645

Palmstrom A (1974) Characterization of jointing density and the quality of rock masses (in Norwegian). Internal report, A.B. Berdal, Norway, 26 p

Panda MK, Mohanty S, Pingua BMP, Mishra AK (2014) Engineering geological and geotechnical investigations along the head race tunnel in Teesta stage-III hydroelectric project, India. Eng Geol 181:297–308

Quiñones-Rozo C (2010) Lugeon test interpretation, revisited. In: Collaborative management of integrated watersheds. US Society of Dams, 30th Annual Conference. pp 405–414

Rahimi B, Shahriar K, Sharifzadeh M (2014) Evaluation of rock mass engineering geological properties using statistical analysis and selecting proper tunnel design approach in Qazvin-Rasht railway tunnel. Tunn Undergr Space Technol 41:206–222

RockWare Inc. (2009) RockWorks. [software]. RockWare, Incorporation, Golden

Turkmen S (2003) Treatment of the seepage problems at the Kalecik Dam (Turkey). Eng Geol 68:159–169

Ukstins I, Renne P, Wolfenden E, Baker J, Ayalew D, Menzies M (2002) Matching conjugate volcanic rifted margins: 40Ar/39Ar chronostratigraphy of pre- and syn-rift bimodal flood volcanism in Ethiopia and Yemen. Earth Planet Sci Lett 198:289–306

UNESCO (1976) Engineering geological maps: a guide to their preparation. The UNESCO Press, Switzerland 76 pp

Uromeihy A (2000) The Lar Dam; an example of infrastructural development in a geologically active karstic region. J Asian Earth Sci 18:25–31

Walraevens K, Vandecasteele I, Martens K, Nyssen J, Clymans W, Moeyersons W, Gebreyohannes T, De Smedt F, Poesen J, Deckers J, Van Camp M (2009) Groundwater recharge and flow in a small catchment in the Tigray region in North Ethiopia. Hydrol Sci J 54(4):739–753

Yazew E (2005) Development and management of irrigated lands in Tigray, Ethiopia. Taylor and Francis, London